ORGANOMETALLICS

Article

pubs.acs.org/Organometallics

Luminescent Conjugates between Dinuclear Rhenium Complexes and Peptide Nucleic Acids (PNA): Synthesis, Photophysical Characterization, and Cell Uptake

Cristina Mari,[†,⊥] Monica Panigati,*[,†] Laura D'Alfonso,[‡] Ivan Zanoni,[§] Daniela Donghi,[†,⊥] Laura Sironi,[‡] Maddalena Collini,[‡] Stefano Maiorana,[†] Clara Baldoli,[∥] Giuseppe D'Alfonso,[†] and Emanuela Licandro*[,†]

[†]Dipartimento di Chimica, Università degli Studi di Milano, via Golgi 19, I-20133 Milano, Italy

[‡]Dipartimento di Fisica, Università di Milano-Bicocca, piazza della Scienza 3, I-20126 Milano, Italy

[§]Dipartimento di Biotecnologie e Bioscienze, Università di Milano-Bicocca, piazza della Scienza 2, I-20126 Milano, Italy

[∥]Istituto di Scienze e Tecnologie Molecolari, CNR, Via C. Golgi 19, I-20133 Milano, Italy

Supporting Information

ABSTRACT: Different PNA decamers have been appended to a luminescent $[Re_2(\mu\text{-}Cl)_2(CO)_6(\mu\text{-}1,2\text{-diazine})]$ complex, to obtain conjugates suitable for cellular imaging. The new compounds can be dissolved in water in the presence of an amount of DMSO as small as 0.4−0.6 mol %. The conjugation with PNA did not perturb the photoluminescence behavior of the organometallic fragment: emission from ^{3}MLCT excited states, centered at ca. 610 nm, was observed, with satisfactory photoluminescence quantum yields (Φ = ca. 0.01, in aerated water). Moreover, the emission could be stimulated also by two-photon excitation. Experiments of cell uptake, performed with different cell lines and under different experimental conditions, showed that the nature of the PNA oligomer strongly affects the biointeraction, while no major differences were observed among the cell lines investigated. The Re-PNA conjugates containing neutral PNA decamers (either homothymine or a standard sequence of the four nucleobases) showed a marked tendency to concentrate in the nuclear region, whereas nucleus penetration was more difficult for the free dirhenium complex. Staining of nucleus and cytoplasm with different colors was generally observed. No nucleus penetration was instead observed for a water-soluble Re-PNA homothymine decamer end-capped with four lysine residues, which localized in endosome-like compartments.

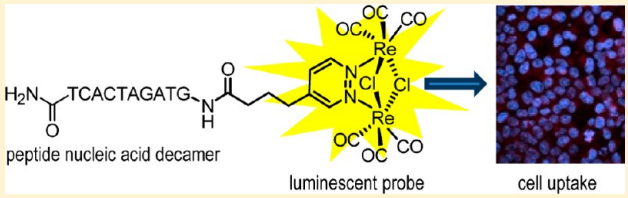

INTRODUCTION

The definition of bioorganometallic chemistry as a specific research area, stated since 1985,[1,2] has definitely established the importance and utility of combining organometallic complexes with organic systems and biomolecules.[3,4] The huge number of papers and studies in this field witness the innovative contributions to the development of several research topics, such as environmental science, toxicology, biosensors, radiopharmaceuticals, natural and artificial enzymes, and bioanalysis.[3−5]

Many metal complexes present suitable spectroscopic, photophysical, and electrochemical properties that can be used in diagnosis and therapy. The conjugation of a metal center with a biomolecule can generate bioconjugates with peculiar features, in which the original properties of both the organometallic moiety and the biomolecule are retained or enhanced by a synergistic interaction, with great benefit for biological purposes.[3−5]

In the last few years, the use of d^6 transition-metal complexes conjugated to biomolecules as luminescent probes in fluorescence cell microscopy has steadily grown.[6] Among them, tricarbonyl Re(I) diimine complexes appear very promising for application in bioimaging. The most explored complexes have the general formula $[Re(CO)_3(N^\wedge N)(PyR)]^x$, where N^N indicates a bipyridine-like chelating ligand, PyR a substituted pyridine, and the charge x is usually positive or negative, according to the nature of the N^N ligand. They emit from triplet metal-to-ligand charge transfer states (^{3}MLCT) and show photophysical properties suitable for biological applications, such as satisfactory photoluminescence quantum yields in aqueous media and in the presence of oxygen, large Stokes shifts, relatively long lifetimes, and high sensitivity not only to the ligand sphere but also to the local surroundings,[7] such as hydrophobicity of the environments.[8,9]

Because of these features, a large number of mononuclear Re(I) complexes have been synthesized and used as luminophores in fluorescence cell imaging.[10,11] In most cases, specific groups have been introduced in the ligand sphere, in order to interact with, or bind to, biological targets,[12] while only

Special Issue: Organometallics in Biology and Medicine

Received: May 23, 2012
Published: July 25, 2012

dx.doi.org/10.1021/om3004515 | Organometallics 2012, 31, 5918−5928

a few reports concerned the uptake and localization in human cells of unfunctionalized $Re(CO)_3(N^\wedge N)$ complexes.[13]

Peptide nucleic acid (PNA) is a DNA mimic,[14] in which *N*-(2-aminoethyl)glycine units form a pseudopeptide chain bearing the four nucleobases (Chart 1). Because of its neutral chain, PNA exhibits stronger and more selective binding affinity for complementary nucleic acid (DNA and RNA) strands than natural nucleic acids. PNA also shows higher mismatch selectivity and noticeable chemical and enzymatic stability in comparison to natural oligonucleotides. The above advantages have addressed many research efforts to the use of PNA for DNA detection, by providing PNA of appropriate analytical probes. For this purpose different metal complexes have been conjugated to PNA oligomers,[15] with the aim of giving them new biochemical and spectroscopic properties (electrochemical, fluorescent, radioactive, etc.).[16−21]

Chart 1. Schematic Drawing of a Peptide Nucleic Acid (PNA) Oligomer and Its Hybridization with Complementary DNA

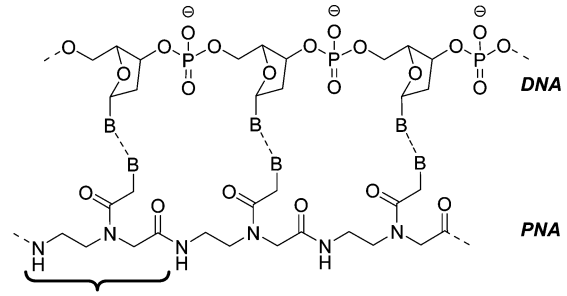

Some examples of rhenium-PNA conjugates have been reported in the literature,[22−24] but only one of them concerned a luminescent species.[22] Moreover, we have recently preliminarily communicated the use of a new neutral luminescent dirhenium(I) complex (**1**; Chart 2), covalently conjugated to a homothymine PNA decamer (**2**), as a suitable fluorophore for cell imaging.[25]

Complex **1** belongs to a recently discovered family of luminescent rhenium complexes, constituted of two $Re(CO)_3$ units joined by a bridging pyridazine ligand and two ancillary anionic ligands (typically halogens).[26,27] Like the mononuclear $Re(CO)_3(N^\wedge N)$ complexes, these dinuclear species emit from ^{3}MLCT excited states, but at variance with their mononuclear counterparts, some of these neutral complexes exhibit very high photoluminescence quantum yields (up to 0.5), both in deaerated solutions (in apolar solvents)[28] and in the solid state.[29,30]

Chart 2. The Dinuclear Re(I) Complex 1 and Its Homothymine-PNA Coniugate 2

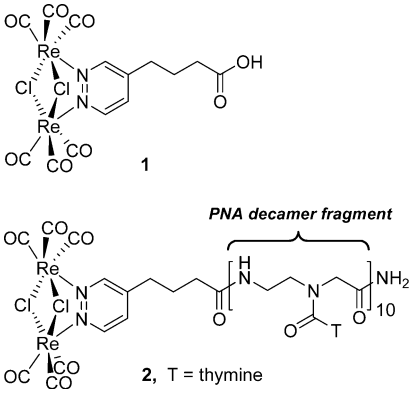

Fast uptake of complex **1** and conjugate **2** (Chart 2) by a prototypical immortal cell line (HEK-293) was observed in aqueous solutions containing a small amount of DMSO (0.6 mol %).[25] Peculiar features of this system were the different color of the emission from the nucleus with respect to cytoplasm and the possibility of stimulating the emission by two-photon excitation (TPE), at wavelengths which allow deeper tissue penetration and lower damage to cell tissues.

Now we have undertaken a more systematic study, in which the systems (fluorophores, cell lines) and the experimental conditions (DMSO concentration, temperature, reaction medium) have been varied, in order to obtain a deeper understanding of the uptake process and check the generality of the results. A new dinuclear Re(I) complex containing an aliphatic amide substituent on the diazine ligand (complex **3**, Scheme 1) has been prepared, to obtain a model more reliable than **1** of the organometallic fragment which is present in the Re-PNA conjugates and also to eliminate the negative charge generated by ionization of the carboxylic group of **1** at physiological pH. To investigate the effect of the nature of the PNA oligomer, a new Re-PNA conjugate (**4**, Scheme 2) has been synthesized, with a PNA decamer sequence (GTAGAT-CACT) containing all four nucleobases. Moreover, a Re-homothymine PNA decamer endowed with four lysine residues as a hydrophilic tail (bioconjugate **5**) has been synthesized, because it has already been shown that conjugation of a suitable positively charged peptide residue[31] to PNA is a valuable strategy for improving both water solubility and cell penetration of PNAs.

The photophysical characterization of the new fluorophores and their cell uptake experiments under different conditions by different cell types are described. The effects of the nature of the complexes and of the experimental conditions have been investigated by using HEK-293 cells, but a preliminary investigation of the effect of the nature of the cell line has also been performed, to exclude that possible differences among the fluorophores were due to cell intrinsic behaviors. The B16 melanoma tumor cell line and a primary cell culture of macrophages were used toward this aim. In particular, freshly derived macrophages gave us the possibility to test our complexes with cells of the innate immune system, which constantly patrol different tissues and are known to be very efficient in the uptake of various molecules.

RESULTS AND DISCUSSION

Synthesis of Complex 3 and of the Re-PNA Conjugates 4 and 5. The new complex **3** (Scheme 1), which is an air-stable yellow solid, was prepared in good yield by refluxing, in toluene solution, the *N*-propyl-4-(pyridazin-4-yl)butanamide ligand with 2 equiv of $[Re(CO)_5Cl]$. The ligand was in turn obtained by treating 4-(pyridazin-4-yl)butanoic acid with an excess of propan-1-amine in the presence of DCC as condensing agent, at room temperature in CH_2Cl_2 as solvent.

The new dinuclear rhenium(I) PNA decamer conjugates **4** (Scheme 2) and **5** (Chart 3) were prepared through a synthetic procedure modified with respect to that used for the synthesis of conjugate **2**.[25] The previous method was based on the automated solid-phase synthesis of the PNA decamer, using

dx.doi.org/10.1021/om3004515 | *Organometallics* 2012, 31, 5918−5928

Scheme 1. Synthetic Route to Complex 3

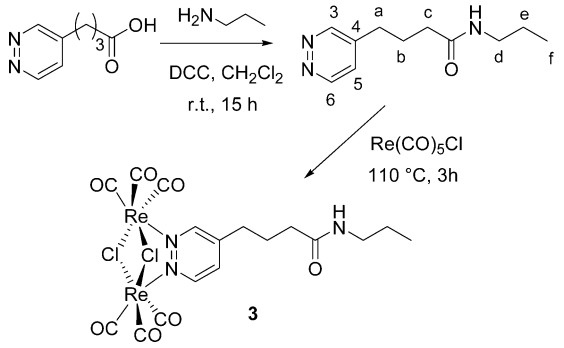

standard Boc-procedure conditions (see the Experimental Section), followed by coupling of the diazine ligand and finally by the reaction with an excess of $[Re(CO)_5Cl]$, in refluxing toluene. This methodology failed for the synthesis of **4**, in which PNA contains the four nucleobases in the standard GTAGATCACT sequence (ST-PNA). Indeed, MALDI-TOF analysis of the crude reaction mixture, after cleavage from the resin, revealed the presence, in addition to the desired product, of several conjugates with higher molecular weights. These latter species can reasonably arise from the complexation of "$Re(CO)_3$" fragments on guanine bases present in the PNA sequence. Indeed, it has already been reported that rhenium tricarbonyl moieties are able to coordinate the N7 of guanine,[32] and complexes of the general formula $[Re(guanine)_2X(CO)_3]$ were recently reported by Alberto and co-workers.[33,34] The ability of "$Re(CO)_3$" fragments to coordinate to guanine nucleobases, under our reaction conditions, has been confirmed by reacting a guanine-containing PNA monomer (mon-G), anchored on the resin, with $Re(CO)_5Cl$ in refluxing toluene for 3 h. After cleavage from the resin, ESI mass spectrometry revealed the presence of three peaks with molecular weights of 887.2, 579.2, and 309.2, attributable to $[(mon\text{-}G)_2Re(CO)_3]^+$, $[(mon\text{-}G)Re(CO)_3]^+$ and $[mon\text{-}G]^+$, respectively.

Chart 3. Schematic Drawing of Re-PNA Conjugate 5

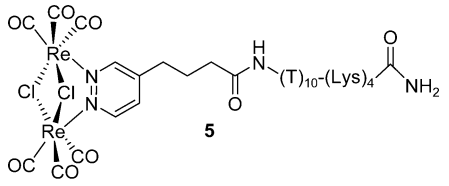

Therefore, two more reliable methods for the synthesis of **4** were investigated (Scheme 2). In the first one (route A), we reacted the diazine ligand, already inserted at the end of the PNA sequence, with a dinuclear Re(I) complex containing a labile oxadiazole bridging ligand, namely $[Re_2(\mu\text{-}Cl)_2(CO)_6(\mu\text{-}ppd\text{-}\kappa N3{:}\kappa N4)]$ (ppd = 2,5-diphenyl-1,3,4-oxadiazole).[35] The reaction, performed in toluene solution at 90 °C, afforded, after cleavage from the resin, the desired conjugate **4**, but with unsatisfactory yields (always lower than 10%).

The second synthetic methodology (route B) involved the reaction of the preformed complex **1** with the amine terminal of the standard sequence of PNA decamer supported on the resin, using HATU as condensing agent and DIPEA, in NMP as solvent, to form the amide bond. Cleavage from the resin, under the usual acidic conditions, gave a yellow luminescent crude product, from which the bioconjugate **4** was isolated by RP-HPLC purification. A MALDI-TOF mass spectrum confirmed the presence of the expected compound. In this case, the isolated yield of **4** increased to ca. 35%.

The same method proved to be suitable also for the synthesis of conjugate **5**, constituted of a homothymine PNA decamer endowed with four lysine residues as a hydrophilic tail (Chart 3).

Using this approach, the conjugate **2** could also be obtained more efficiently than with the previously reported method.[25]

Photophysical Studies. It has been previously shown[25,26] that photoluminescence, in complex **1** and more generally in the whole family of dinuclear Re-diazine complexes, originates from $d\pi(Re)-\pi^*(diazine)$ triplet metal-ligand-to-ligand charge transfer excited states (^{3}MLLCT). Several arguments support

Scheme 2. Synthetic Routes to Re-PNA Conjugate 4: Routes A and B

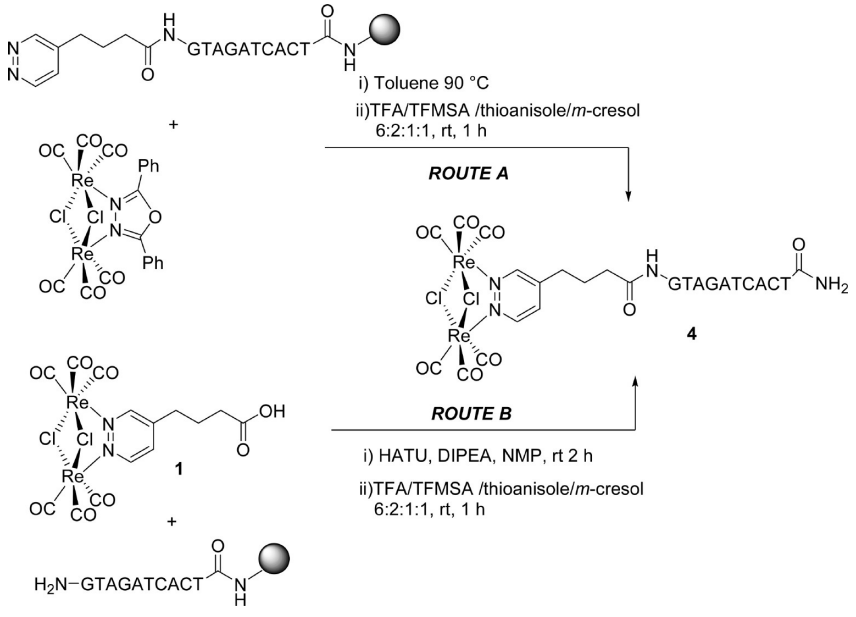

dx.doi.org/10.1021/om3004515 | Organometallics 2012, 31, 5918–5928

this attribution: the solvent effect on the energy and on the intensity of the emission, the quenching of the emission in the presence of O_2, the effect of the diazine substituent on the emission energy, and the fair correlation between this value and the electrochemical gap, with a slope close to unity.[25−27]

Here we have investigated the photophysical properties of complex **3** and of the Re-PNA conjugates **2**, **4**, and **5** in two different media: water/acetonitrile 1/1 solution and water (pure for **5**, with a small amount of DMSO added for the other species).

In water/acetonitrile the new complex **3** and the new conjugate **5** showed photophysical behaviors very similar to those of **1** (λ_{em} 610 nm, Φ = 0.014) and of the conjugate with homothymine PNA-decamer **2** (see Table 1).[25] The conjugate

Table 1. Photophysical Properties of Complexes 2−5 at 298 K in Aerated Solutions[a]

	H_2O/MeCN 1/1 v/v			H_2O/DMSO[b]
compd	λ_{em}/nm	Φ	τ/ns	λ_{em}/nm (amt of DMSO/%)
2	611	0.016[c]	316	602 (1.5)
3	607	0.012	216	607 (3.5)
4	604	0.006	190[d]	571 (1.5)
5	607	0.015	270	610 (0)

[a]Samples were excited at 330 nm. Emission spectra were corrected for the emission spectral response (detector and grating) using the standard correction curves. [b]All measured in 3 μM solution, except for **5** (5 μM). [c]The Φ value for conjugate **2** is higher than that previously reported,[25] since it has been determined using the revised value for the emission of $[Ru(bpy)_3]Cl_2$ in water.[36] [d]A second faster component (48 ns) accounting for 6% of the emission has been measured.

containing the PNA standard sequence **4** showed a broad emission band centered about in the same position (604 nm), but with slightly lower photoluminescence quantum yields (Φ = 0.006) and shorter lifetime.

This (moderate) quenching effect might result from an intramolecular electron transfer (ET) process from a guanine base to the excited state of the complex, as previously observed for several Ru(II)[37] and Re(I) complexes.[38] Electronic conditions must be fulfilled to allow such photoinduced electron transfer: the reduction potential of the excited state of the complex must be higher than the reduction potential of the G^+/G couple, and the orbitals involved in the electronic transitions have to be the same involved in the electrochemical reduction and oxidation processes. The reduction potential of the excited state can be calculated as the sum of the ground-state reduction potential and the energy transition from the thermally equilibrated excited state to the zero vibrational level of the ground state (E_{00}).[39] The latter term, in turn, can be estimated to lie between the intersection of the excitation and emission spectra (ca. 500 nm, 2.48 eV) and the emission maximum (604 nm, 2.05 eV).[38c] Due to the practical difficulties (the available amount of **4** was not sufficient to perform the cyclic voltammetric characterization), we measured the oxidation and the reduction potential of the parent complex **1**, reasonably assuming that the redox properties of **4** do not significantly differ from those of **1**. Indeed, the redox processes involve the Re_2-diazine moiety only, which, in the presence of the spacing alkyl chain, is not electronically coupled with the PNA moiety. The CV analysis of **1** (see Figure S1 in the Supporting Information) showed a monoelectronic reduction peak, located at −0.79 V vs NHE, which is both chemically (symmetrical return peak, stable products) and electrochemically reversible (ca. 57 mV half peak width and almost 0 E_p vs log ν slope). The reduction process is located on the pyridazine ligand, in agreement with the electrochemical behavior observed for many other complexes of this family.[26−28] The oxidation process, bielectronic and irreversible (both chemically and electronically), appears at 1.88 V vs NHE and, in agreement with what has been reported for the other complexes, can be attributed to a simultaneous two-electron loss from the two metal centers. On the basis of the aforementioned spectroscopic and electrochemical data, the reduction potential of the excited state should lie between 1.69 and 1.24 V (vs NHE): therefore, it is high enough to oxidize the guanine nucleoside, for which $E^\circ[G^{\bullet+}/G]$ = 1.29 V (vs NHE) has been measured.[40]

We have also investigated the photophysical properties of **5** in water solution and of compounds **2**−**4** in water containing a small amount of DMSO, due to their very poor solubility in pure water (see Table 1). A very low fraction of DMSO (1.5% v/v) was enough to dissolve the conjugates **2** and **4** (giving a final 3 μM concentration), whereas for complex **3** clear solutions were obtained only with a higher (3.5% v/v) concentration of DMSO. Interestingly, these clear solutions displayed emission at 590 nm, which shifted to 607 nm upon heating at 40 °C for 30 min. This suggests that the initially formed solutions contained visually undetectable micro-/nanoparticles of precipitate, because a hypsochromic shift on going from fluid solution to the solid state is a general feature of these MLCT emitters.[26,29] Actually, the solid-state emission spectra of **1** and **2** showed maxima at 530 and 555 nm, respectively.

The emission of conjugate **4** in water/DMSO 1.5% was strongly blue-shifted (by about 30 nm) with respect to that observed in water/acetonitrile solution (λ_{max} 571 vs 604 nm). This cannot be explained by polarity arguments (water is a more polar solvent than acetonitrile and DMSO,[41] and a red shift on increasing solvent polarity is expected for emission from charge-transfer excited states)[42] and might rather be attributable to the conformational arrangement in the water/DMSO solution of the PNA chain, which could fold back and wrap around the metal complex, shielding it from the polar solvent.[43] A variable-temperature measurement showed a significant increase of the intensity of the emission upon cooling (ca. 90%), with a small hypsochromic shift (from 573 nm at 40 °C to 568 nm at 5 °C; Figure 1).

In order to confirm this hypothesis, we performed analogous variable-temperature experiments using complex **3** and the homothymine conjugate **2**, showing in both cases a much smaller increase of the emission intensity in the same temperature range used for **4** (25% for **3** and 30% for **2**; Figures S2 and Figure S3 in the Supporting Information), without any significant shift of the maximum. Also, the blue shift of the emission with respect to the water/acetonitrile solution was much less pronounced for **2** (from 611 to 602 nm) and was not observed at all for **3** (see Table 1).

The different behaviors observed for the two Re-PNA conjugates **2** and **4** should therefore be attributed to different conformations adopted in water by the two PNA chains around the Re(I) complex. Indeed, it has already been evidenced that the propensity of PNA oligomers to self-organize and aggregate in solution is particularly pronounced for PNAs bearing some self-complementarity (such as the well studied PNA H-GTAGATCACT-L-Lys-NH_2, which contains the same se-

dx.doi.org/10.1021/om3004515 | Organometallics 2012, 31, 5918−5928

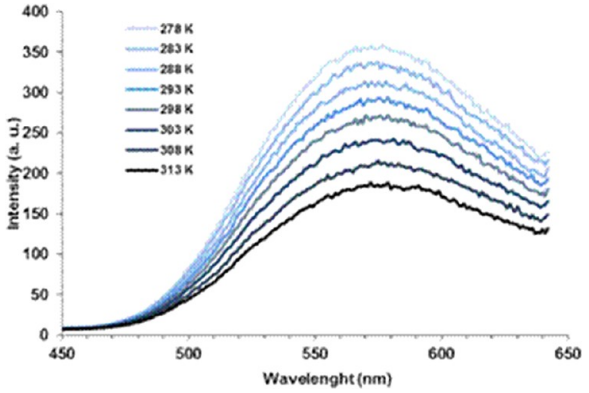

Figure 1. Variable-temperature photoluminescence spectra for **4** (λ_{ex} 330 nm), recorded in water solution containing DMSO 1.5% v/v, starting from 313 K and progressively cooling to 278 K.

quence present in **4**).[44] Therefore, we can assume that in the case of **4** the metal complex is embedded inside a three-dimensional interstrand network, formed through nucleobase interactions, and is therefore somewhat shielded from the aqueous environment. This hypothesis is also in agreement with its more difficult cellular uptake (see below) and with the fluorescence microscope images, which show luminescent aggregates floating in the well of the plate (see Figure S4 in the Supporting Information). In contrast, in the case of **2** a simple fold-back of the PNA chain might be responsible for the moderate hypsochromic shift that is observed.

The photoluminescence of **5** was measured in pure water solution, due to its higher solubility. The emission was slightly modulated by the concentration, and the wavelength of the maximum shifted from 610 to 595 nm on increasing the concentration from 5 to 50 μM. This moderate blue shift is probably due to the amphiphilic nature of this Re-PNA conjugate, which in water tends to self-assemble in micellar-like systems, with the lysine residues exposed toward the water environment and the Re(I) complexes embedded in the core. A similar behavior has been reported for PNA amphiphiles, obtained by attaching an *n*-alkane and natural amino acids (such as lysines) at the opposite ends of a PNA sequence.[45] DLS measurements performed on the 50 μM solution confirmed the presence of nanoaggregates, with hydrodynamic diameters ranging from 20 to 200 nm.

Cell Uptake. We have recently reported that complex **1** and its conjugate **2** are able to penetrate the cellular membrane of HEK-293 cells, staining both the cytoplasm and the nucleus with different colors. These experiments were performed using a small amount of DMSO (2.5% v/v, i.e. 0.6% mol), to increase the solubility of **1** and **2**. It was determined that neither the free complex **1** nor the conjugate **2** showed any specific toxicity under these conditions.[25]

Here we have investigated first of all the behavior of complex **3** and of conjugate **4** under the same experimental conditions of the previous work, in order to evaluate if a different functional group on the diazine moiety or a different PNA sequence could modify their uptake and/or their localization inside the cells.

Small aliquots (50 μL) of a 0.12 mM DMSO solution of the proper luminescent probe were added to 2 mL of phosphate buffer solution (PBS) or of Dulbecco's modified Eagle's Medium (DMEM, used in the experiments requiring longer incubation times) in different wells of the plate containing HEK-293 cells, giving a 3 μM concentration of each sample in the wells, with a resulting concentration of DMSO of 2.5% v/v. Two-photon excitation at 770 nm was employed for the acquisition of the microscope images, since it has been previously shown that both the parent complex **1** and the homothymine conjugate **2** are able to emit upon two-photon excitation.[25] The luminescence of the complex was detected in a wide spectral range, through 485/30, 535/50, and 600/40 band-pass filters. Measurements performed under the same laser power in the absence of the complexes showed that cell autofluorescence was negligible.

The images clearly showed that the conjugate **4** was taken up by the cells, even if a longer incubation time was required (about 80 min), with respect to the experiments previously described with **1** and **2**, in PBS (containing the same 2.5% v/v concentration of DMSO).[25] At the beginning of the experiments large luminescent aggregates were observed (as discussed above; see Figure S4 in the Supporting Information), which slowly disappeared. The emission from the cytoplasm was detectable in the red channel only, whereas the nuclei were well imaged in all the channels (Figure 2) as in the case of conjugate **2**.[25]

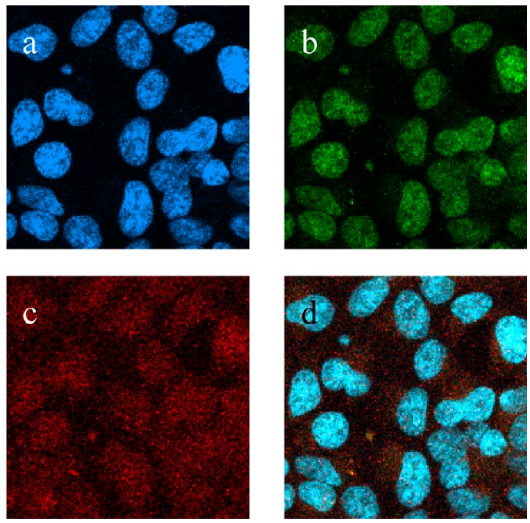

Figure 2. TPE luminescence images of HEK-293 cells incubated with a 3 μM solution of **4** for 80 min in DMEM containing DMSO 2.5% v/v, at 37 °C, through 600/40 (a), 535/50 (b), and 485/30 (c) band-pass filters and their superposition (d). The field of view was 72 × 72 μm^2, cropped from a 230 × 230 μm^2 image.

Since in this experiment the incubation medium was different from PBS, used in the previous set of experiments,[25] we checked that the uptake of **2** was much faster than that of **4**, also using DMEM: after 6 min the nuclei of the cells were stained with an intense blue-green color, while the cytoplasm gave a weaker red emission (see Figure S5 in the Supporting Information). In both cases the images clearly enlightened the chromatin distribution inside the nucleus.

A different behavior was observed for complex **3**. Even if it was not completely dissolved in water with 2.5% DMSO (see above), **3** was able to cross the cellular membranes, but in this case staining of the cytoplasm was clearly detectable in the red channel (and to a lesser extent in the green one), while weaker emission from the nucleus was recognized only in the blue channel. The emission from the nucleus was more clearly detectable at longer times (Figure 3).

dx.doi.org/10.1021/om3004515 | *Organometallics* 2012, 31, 5918−5928

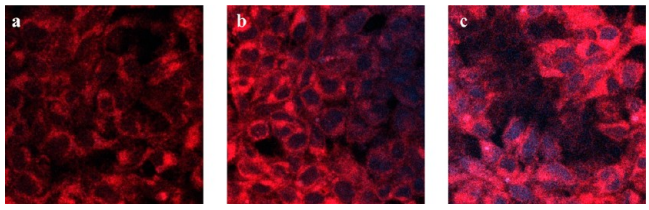

Figure 3. TPE luminescence images of HEK-293 incubated with 3 μM solution of **3** in DMEM containing DMSO 2.5% v/v, at 37 °C, for 5 min (a), 30 min (b), and 60 min (c). The images were visualized through 600/40 and 485/30 band-pass filters. The field of view was 460 × 460 μm^2. See Figures S6 and S7 in the Supporting Information for the images visualized through the three separate channels.

The presence of DMSO in the incubation medium deserves some comment. Its use was necessary for increasing the solubility of the complexes and of the Re-PNA conjugates. However, it is known that DMSO has the ability to induce cell fusion and cell differentiation and to enhance the permeability of lipid membranes. It exhibits distinct modes of action, over different concentration ranges. In particular, at low concentrations (up to 10 mol %), DMSO induces membrane thinning, resulting in an enhancement of the fluidity of the membrane's hydrophobic core and allowing the internalization of a higher amount of hydrophobic molecules.[46] At higher concentrations, DMSO induces transient water pores into the membrane. At even higher concentrations, individual lipid molecules are desorbed from the membrane, followed by disintegration of the bilayer structure.[46a] The DMSO concentration used in this study is extremely low (0.6 mol %), so that any macroscopic damage of the membrane structure can be ruled out.

However, to get a deeper insight into the role of DMSO in the uptake process, we performed experiments using a smaller amount of DMSO (1.5% v/v, corresponding to 0.4 mol %), without varying the nominal chromophore concentration (3 μM, although the "effective" concentration was certainly smaller in the case of **3**, due to its partial dissolution with such a small amount of DMSO). Under these conditions the three investigated dyes **2**–**4** showed three different behaviors. No uptake of **4** was observed. This is likely due to the formation of the aforementioned aggregates (clearly recognizable in the two-photon excitation images), which, in the presence of a reduced amount of DMSO, are unable to cross the membranes. In contrast, complex **3** and the Re-PNA conjugate **2** were internalized inside the cells, but with quite different features. Complex **3** stained almost immediately (3 min) the cytoplasm of all the cells, and no staining of the nucleus was observed, even for longer incubation time (up to 30 min; see Figure 4a), whereas staining of both the nucleus and cytoplasm was observed for **2**, but without the clear differentiation of the two environments, as in the experiments with 2.5% of DMSO (see Figure 4b).

Experiments have also been performed at low temperature (ca. 4 °C) for all the species **2**–**4**, with DMSO concentrations of both 2.5 and 1.5% v/v. No significant difference was observed with respect to the data obtained at 37 °C, indicating that endocytotic transport mechanisms do not play a major role in this process.

Finally the behavior of the water-soluble Re-PNA conjugate **5**, containing four lysine residues, was investigated in water solution, without any added DMSO. The conjugation with the positively charged peptide residue is expected not only to enhance the water solubility of PNA but also to promote the

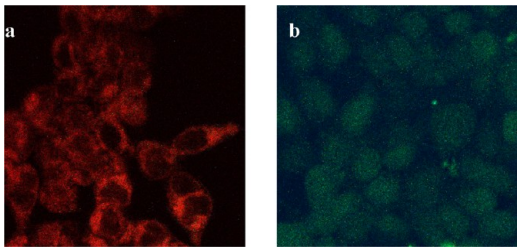

Figure 4. TPE luminescence images of HEK-293 cells incubated in PBS, containing DMSO 1.5% v/v, at 37 °C with (a) 3 μM solution of **3** for 20 min and (b) 3 μM solution of **2** for 30 min. The images are the superimposition of all the band-pass filters. The field of view was 184 × 184 μm^2.

cell uptake and, possibly, to enhance recognition of nucleic acid targets inside the cells.[47] Not surprisingly, the cell uptake and the localization of conjugate **5** were significantly different with respect to the other conjugates. It easily penetrated the HEK-293 cells, even at low temperature, in agreement with what was already reported for different PNA oligomers endowed with terminal lysine moieties.[47] However, it was not homogeneously spread inside the cytoplasm but rather localized in small globular endosome-like compartments, giving the punctuate luminescence shown in Figure 5. This segregation, indicative of

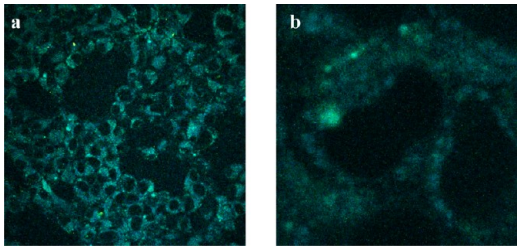

Figure 5. TPE luminescence images of HEK-293 cells incubated with a 3 μM solution of **5** in PBS at 37 °C: (left) complete image; (right) 6× zoom of some cells. Field of view: (a) 230 × 230 μm^2; (b) 39 × 39 μm^2.

the occurrence of an endocytosis-like internalization (different from what was observed for the other conjugates), is clearly attributable to the presence of the lysine fragments, since the same localization has been reported for different PNA oligonucleotides conjugated with short oligolysine tails.[15,47] An experiment at 4 °C showed a slower uptake, confirming the occurrence of a metabolism-dependent process. No staining of the nucleus was detected, in agreement with the strong localization of the probe in specific subcellular compartments. Interestingly, the addition of 2.5% of DMSO in the incubation medium did not modify this localization and no staining of the nucleus was observed, even after 30 min. This suggests that the lack of nuclear staining observed in this case arises from the nonhomogeneous distribution of the luminescent probe inside the cytoplasm (as observed in the cases of conjugates **2** and **4**). Therefore the presence of DMSO, when used, is not sufficient by itself to increase the nuclear membrane permeability. Moreover, differently from **2** and **4**, the emission from the cytoplasm was detectable on the green and blue channels only.

Preliminary uptake experiments with a different cell line, namely mouse melanoma tumor cells, have also been performed on compounds **2**–**4**, to evaluate the generality of the behavior observed with HEK-293. The experiments were

dx.doi.org/10.1021/om3004515 | *Organometallics* 2012, 31, 5918–5928

performed as described above for HEK-293 cells, with a concentration of DMSO of 1.5% v/v. Under these conditions only complex **3** was able to penetrate the cellular membranes, localizing mainly in the cytoplasm and in the perinuclear region, while the nucleus was only moderately stained. At variance with what was observed with HEK-293 cells, in this case no difference of wavelength was observed in the emission coming from the cytoplasm and the nucleus, the intensity decreasing on going from the red to the green to the blue channels (see Figure 6). In contrast, conjugate **2** showed a moderate uptake

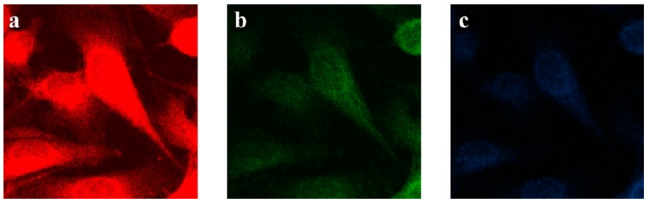

Figure 6. TPE luminescence images of human melanoma cells incubated with a 3 μM solution of **3** in PBS containing DMSO 1.5% v/v, at 37 °C, for 6 min through 600/40 (a), 535/50(b), and 485/30 (c) band-pass filters. The field of view was 184 × 184 μm^2.

with a weak diffuse green fluorescence from cytosol and nucleus. No stained cells were detected using conjugate **4**, due to the formation of aggregates, again visible in the TPE images.

Finally, uptake experiments have been performed using a primary cell culture of macrophages. The selected incubation medium was DMEM, and the concentration of DMSO was set at 2.5%. The results were very similar to those obtained in the case of the HEK-293 cells under the same conditions. Complex **3** and conjugate **2** displayed a good uptake, which was significantly faster for **3**. A marked distinction of the emission color between nucleus and cytoplasm was still detectable, rapidly for **3** and at longer times for **2** (see Figures 7 and 8, respectively). In contrast, once again the conjugate **4** was unable to stain the cells. In this case an additional aggregation source could derive from the presence in the incubation

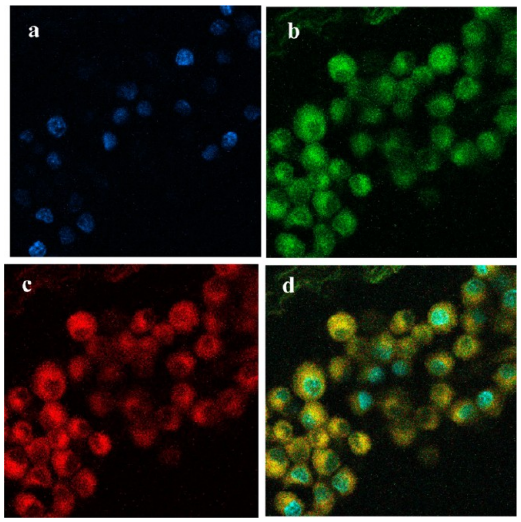

Figure 7. TPE luminescence images of macrophages incubated with a 3 μM solution of **3** in DMEM containing DMSO 2.5% v/v, at 37 °C, for 11 min, through 485/30 (a), 535/50 (b), and 600/40 (c) band-pass filters and their superposition (d). The field of view was 230 × 230 μm^2.

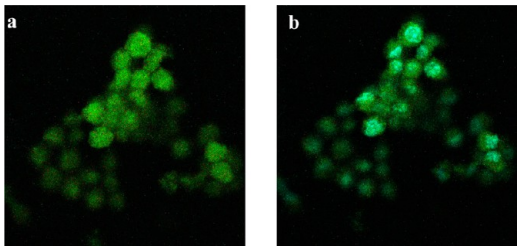

Figure 8. TPE luminescence images of macrophages incubated with a 3 μM solution of **2** in DMEM containing DMSO 2.5% v/v, at 37 °C, for 27 min (a) and 47 min (b). The field of view was 230 × 230 μm^2. See Figures S8 and S9 in the Supporting Information for the images visualized through the three separate channels.

medium of metabolic products of macrophages, such as proteins of the HMGB family, known to be able to recognize, bind, and interact with different nucleic acids[48] and therefore also with PNAs. This could result in a reduced availability of **4** for the cell uptake.

The results so far presented show a variegated picture of the penetration ability of the investigated compounds. Significant differences have been observed not only between the cationic (**5**) and the neutral (**2** and **4**) conjugates but also between the two neutral species. The more difficult uptake of **4** with respect to **2** is probably attributable to the tendency of the standard nucleobase sequence of **4** to give interstrand interactions, resulting in the formation of large aggregates that reduce the availability of **4** for cell uptake.

The internalization of the cationic conjugate **5**, bearing four lysine residues, occurs most likely by an endosome-mediated pathway. The conjugate appears to be trapped in endosome-like compartments, and it is not able to diffuse in the cytoplasm or penetrate the nucleus. This behavior has been observed for other PNAs conjugated to cell-penetrating peptides,[15,31,47] even if nuclear localization has also been reported.[31]

The opposite occurs for the complex **3** and the neutral conjugates **2** and **4**, for which the available data suggest that endocytotic mechanisms do not have primary importance, also due to the presence of the (small, ca. 0.5% mol) amount of DMSO present in the medium, leading to homogeneous distribution inside the cytoplasm. The role of DMSO in membrane fluidification is confirmed by the more difficult uptake of **2**–**4** on lowering the DMSO concentration.

Moreover, the two conjugates **2** and **4** show a marked tendency to concentrate in the nucleus. For complex **3** nuclear staining appears to be more difficult (apart from the case of the macrophages). This could suggest a specific role of the PNA chain in favoring transport within the nucleus. Otherwise, in agreement with literature data, an enhancement of membrane permeability caused by the higher concentration of **2** and **4** in the incubation medium can be hypothesized, due to their higher solubility with respect to that of **3**. This effect was already reported not only for PNA derivatives[47a] but also for metal complexes.[49,50]

■ CONCLUSION

The rhenium-based fluorophores presented in this work show several appealing features for cell imaging. Many of these features arise from the peculiar dinuclear molecular structure of the organometallic emitter, characterized by a stiff "Re(μ-Cl)$_2$Re" skeleton, which leads to high photoluminescence quantum yields in solution,[26] allowing imaging with a reduced

dx.doi.org/10.1021/om3004515 | *Organometallics* 2012, 31, 5918–5928

concentration (and then a low toxicity) of the chromophores. Moreover, the bridging coordination of the halide ligand reduces their lability,[51,52] which was often responsible for the toxicity of neutral monuclear diimine rhenium chloride complexes.[11]

The cell uptake experiments have confirmed our previous findings[25] and provided more insight into different aspects of the interaction between these kinds of luminescent probes and cells. Cell penetration and staining were strongly influenced by the nature of the compounds used, without major differences between the HEK-293 cells (more deeply studied) and the other cell types preliminarily investigated.

The tendency of these chromophores to stain nucleus and cytoplasm with different colors, which was one of the more striking results of our preliminary investigation, has also been fully confirmed. Several reasons might be responsible for this. Actually, hypsochromic shifts of ^{3}MLCT emission bands can arise either from a less polar or from a more rigid environment; therefore, both the reduced mobility of the metal complex inside the nuclear environment and the more hydrophobic character of this environment, with respect to the cytoplasm, might explain the observed behavior. On the other hand, interactions with DNA cannot be excluded, but they should primarily involve the organometallic complex and not the PNA fragment, since this behavior is displayed also by the free complexes **3** and **1** (reported in the previous communication).[25] A different but likely hypothesis is the formation of some solid phase within the nucleus, due to supersaturation following the concentration of the probe in the restricted nuclear region. It is well-known that in this class of compounds the luminescence is blue-shifted (rigidochromic effect),[7] and often also more brilliant, in rigid phases.[26]

Future work is planned to better evaluate cell uptake and DNA binding properties of these and similar compounds, with increased solubility in water. Only a deep understanding of such behaviors will allow a rational and more efficient design of these promising bioimaging agents.

EXPERIMENTAL SECTION

Materials and Measurements. All reagents were obtained from commercial suppliers and used without further purification, and solvents were deoxygenated and dried by standard methods. Commercially available 1-hexynoic acid and $Re(CO)_5Cl$ were used as received. 4-(Pyridazin-4-yl)-butanoic acid,[25] complex **1**,[25] and the complex $[Re_2(\mu\text{-}Cl)_2(CO)_6(\mu\text{-ppd-}\kappa N3{:}\kappa N4)]$[35] were prepared according to literature procedures.

All the reactions involving the rhenium complexes were performed using Schlenk techniques. Column chromatography was performed using silica gel 60 (70−230 mesh). ^{1}H NMR spectra were acquired on 300 or 400 MHz spectrometers. MS and HPLC-MS spectra were recorded on Advantage Thermofinnigan instruments (ESI source). HRMS spectra were recorded on a Bruker Daltonics ICR-FTMS APEX II instrument. MALDI-TOF analyses were executed on a Bruker Omniflex spectrometer.

Vials with PTFE frits were used as reactors for solid-phase synthesis. Automated solid-phase syntheses were performed with the peptide synthesizer "ABI 433A", equipped with Synthassist 2.0 software for peptide synthesis, according to the Applied Biosystems ABI 433A Peptide Synthesis User's Manual. MBHA resin in a 3 mL reaction vessel was used. HPLC purifications of PNA oligomers were run using a DISCOVERY BIO WIDE PORE C18 reverse-phase analytical column (25 cm × 4.6 mm, 5 μm) and a DISCOVERY BIO WIDE PORE C18 semipreparative column (25 cm × 10 mm, 10 μm).

Synthesis of *N*-Propyl-4-pyridazin-4-ylbutyramide. *N*-Propylamine (49.5 mL, 0.60 mmol) and DCC (34.2 mg, 0.17 mmol) were added to a solution of 4-(pyridazin-4-yl)butanoic acid (25 mg, 0.15 mmol) in dry CH_2Cl_2 (2 mL). The reaction mixture was stirred overnight at room temperature. Then the solution was evaporated to dryness, to remove the excess amine. The residue was treated with CH_2Cl_2 and the suspension filtered to remove DCU. The resulting solution was evaporated to dryness, to obtain the crude product as a brownish solid, which was used for the synthesis of the rhenium complex without any further purification. ^{1}H NMR (CD_2Cl_2, ppm): δ 0.94 (t, 3H, H_f); 1.53−1.57 (m, 2H, H_e); 2.01 (pq, 2H, H_b); 2.21 (t, 2H, H_c); 2.72 (pt, 2H, H_a); 3.20 (t, 2H, H_d); 7.41 (m, 1H, H_5); 9.08 (m, 2H, H_3, H_6).

Synthesis of $[Re_2(\mu\text{-Cl})_2(CO)_6(\mu\text{-}N\text{-propyl-4-pyridazin-4-ylbutyramide}]$ (3). The complex **3** was synthesized with the same procedure previously reported for the synthesis of **1**.[25] The crude product was purified by column chromatography (CH_2Cl_2/*n*-hexane 8/2 as eluent) and precipitated with *n*-hexane, affording a microcrystalline sample, whose purity was assessed by IR, NMR, and elemental analysis (isolated yields 70%). Anal. Calcd for $C_{17}H_{17}Cl_2N_3O_7Re_2$: C, 24.94; H, 2.09; N, 5.13. Found: C, 25.03; H, 2.20; N, 5.02. IR (CH_2Cl_2): ν_{CO} 2051 (mw), 2032 (s), 1946 (s), 1918 (s) cm^{-1}. ^{1}H NMR (CD_2Cl_2, ppm): δ 0.95 (t, 3H, H_f); 1.53−1.58 (m, 2H, H_e); 2.15 (q, 2H, H_b); 2.32 (t, 2H, H_c); 3.02 (t, 2H, H_a); 3.22 (t, 2H, H_d); 7.91−7.93 (dd, 1H, H_5); 9.64−9.69 (m, 2H, H_3, H_6).

PNA Synthesis. Homothymine-PNA and standard sequence-PNA were prepared by solid-phase synthesis by means of an Applied Biosystems ABI 433A Peptide Synthesizer starting from MBHA resin, in a 3 mL reaction vessel on 20 μM scale, using the Boc strategy, according to the solid-phase synthetic protocol reported by Nielsen[14] and following the procedure described in the ABI 433A synthesizer User's Manual.

Homothymine(PNA)$_{10}$-lys$_4$ Decamer. This compound was prepared, as reported below, using a solid-phase synthetic protocol, starting from MBHA resin downloaded with a lysine unit.

Downloading with Lysine of MBHA Resin. MBHA resin 0.5 g (1 g, 0.63 mmol/g, 0.63 mmol) was poured into a 10 mL Teflon vial and swollen in an excess of CH_2Cl_2 with shaking at room temperature for 30 min. The resin was treated with a solution of DIPEA (5% in CH_2Cl_2) with shaking for 3 min and then washed twice with CH_2Cl_2 (5 mL) and dried by suction for 1 min. A solution of Boc-Lys(2-Cl-Cbz)-OH (0.2 mmol) and DIPEA (2 eq, 0.4 mmol, 51.7 mg, 70 μL) in NMP (2 mL) and a solution of HBTU (0.2 mmol, 75.9 mg) in NMP (2 mL) were mixed together, shaken for 2 min, and added to the resin. The coupling reaction was allowed to proceed at room temperature for 4 h with shaking, and then the resin was filtered, washed with NMP (3 × 2 mL), and treated with 5 mL of the capping solution Ac_2O/Py/NMP (1/25/25). The resin was washed with NMP (2 × 2 mL), CH_2Cl_2 (2 × 2 mL), DIPEA 5% in CH_2Cl_2 (2 mL), MeOH (2 mL), and CH_2Cl_2 (3 × 2 mL) and dried after suction, thus giving the MBHA-Lys resin.

Automated Synthesis of the Homothymine (PNA)$_{10}$-lys$_4$. Starting from the MBHA-Lys resin, first three lysine amino acids were loaded, following the procedure reported above, in order to obtain the MBHA-lys$_4$ resin. Then, the 10 aegPNA monomers were coupled using the standard solid-phase synthetic protocol for PNA synthesis, using the automated Applied Biosystems ABI 433A Peptide Synthesizer. To check the oligomerization outcome, a small portion of resin-supported (PNA)$_{10}$-Lys$_4$ was treated as follows: the resin was poured into a fritted syringe, washed with TFA (2 × 100 μL), and then shaken for 1 h with a solution of TFA/TFMSA/thioanisole/*m*-cresol 6/2/1/1 (300 μL). The reaction mixture was then filtered and the resin washed with TFA (4 × 100 μL), collecting the filtrate, which was concentrated under a nitrogen flow. Cold Et_2O (3 mL) was added to the residue; centrifugation of the slurry gave PNA as a white solid, which was washed with Et_2O (8 × 1 mL) and dried. The cleaved PNA was then purified by reverse phase HPLC (gradient from H_2O/CH_3CN, 95/5 to CH_3CN 100% in 60 min, R_t = 10 min) and characterized by MALDI-TOF mass analysis (m/z 3192.7 (M)).

General Procedure for the Synthesis of Rhenium-PNA Conjugates 2, 4, and 5. *Boc Deprotection of the Resin.* The resin containing PNA (100 mg, 0,2 mmol/g, 0,02 mmol) was

dx.doi.org/10.1021/om3004515 | *Organometallics* 2012, 31, 5918−5928

transferred into a fritted syringe and swollen with CH_2Cl_2 (3 mL) with shaking for 1 h. The solvent was filtered, and then the terminal *N*-Boc protecting group was removed by treating the resin twice with a TFA/*m*-cresol 95/5 solution (3 mL) with shaking for 4 min. The resin was then sequentially washed three times with CH_2Cl_2 (2 mL), NMP (2 mL), and CH_2Cl_2 (2 mL) and then with a solution of DIPEA 5% in CH_2Cl_2 (2 × 3 mL) and CH_2Cl_2 (3 × 2 mL).

Coupling Procedure with Complex ***1****.* A solution of HATU (19 mg, 0.05 mmol, 5 equiv) in NMP (500 μL) was added to a solution of complex **1** (41.2 mg, 0.053 mmol, 5.3 equiv) and DIPEA (18 μL, 0.1 mmol, 10 equiv) in NMP (750 μL) in a vial. The resulting brown mixture was shaken for 2 min and then added to the previously deprotected resin. The mixture was shaken for 2 h (600 r/min), and then the resin was filtered and sequentially washed three times with NMP (2 mL) and CH_2Cl_2 (2 mL) and eventually with CH_2Cl_2 (3 × 2 mL).

Substitution Reaction with [Re₂(μ-Cl)₂(CO)₆(μ-ppd-κN3:κN4)]. Three different toluene suspensions, containing typically 20 mg of resin-supported PNA (corresponding to 0.2 mol/g of the diazine ligand) and different amounts of $[Re_2(\mu\text{-}Cl)_2(CO)_6(\mu\text{-ppd-}\kappa N3{:}\kappa N4)]$ (molar ratio complex/PNA 1.3/5) were prepared. The three reaction mixtures were heated at 90 °C for different times (2−8 h). The products of these solid-phase substitution reactions were purified by washing the resin with toluene.

Cleavage of Re-PNA Conjugates ***2****,* ***4****, and* ***5*** *from the Resin.* The resin was washed twice with TFA (200 μL) and filtered, and a TFA/TFMSA/thioanisole/*m*-cresol 6/2/1/1 solution (500 μL) was added. The mixture was shaken for 1 h and then filtered, and the resin was washed with TFA (4 × 200 μL). The cleavage procedure was repeated twice. The collected filtrates were concentrated under a nitrogen flow, diluted with Et_2O (5 mL), and frozen for 1 h. Centrifugation of the slurry gave a pale yellow solid (fluorescent at 366 nm), which was washed with cold Et_2O (5 × 3 mL) and dried to afford the Re-PNA decamers **2**, **4**, and **5**, which were purified by semipreparative RP-HPLC. HPLC eluent for Re-PNA decamers **2**:[25] H_2O + 0.1% TFA/CH_3CN + 0.1% TFA, gradient from 95/5 to 100% CH_3CN + 0.1% TFA in 30 min, R_t = 15.07 min. MALDI-TOF (*m*/*z*): 3439 $[M^+]$. HPLC eluent for Re-PNA decamers **4**: H_2O + 0.1% TFA/CH_3CN + 0.1% TFA, gradient from 95/5 to 100% CH_3CN + 0.1% TFA in 30 min, R_t = 15.07 min. MALDI-TOF (*m*/*z*): 3486 $[M^+]$. HPLC eluent for Re-PNA decamers **5**: H_2O + 0.1% TFA/CH_3CN + 0.1% TFA from 95/5 to 100% CH_3CN + 0.1% TFA in 20 min, R_t = 11.5 min. MALDI-TOF (*m*/*z*): 3951.5 $[M^+]$.

Electrochemical Measurements. The cyclic voltammetric study of complex **1** was performed in HPLC-grade acetonitrile solutions, at 0.25 mM concentration deareated by N_2 bubbling, with 0.1 M tetrabutylammonium hexafluorophosphate ($TBAPF_6$; Fluka) as the supporting electrolyte, at 298 K. The ohmic drop was compensated by the positive feedback technique.[53] The experiments were carried out using an AUTOLAB PGSTAT potentiostat (EcoChemie, The Netherlands) run by a PC with GPES software, at scan rates typically ranging from 0.02 to 10 V s^{-1}. The working electrode was a glassy-carbon electrode, the counter electrode was a platinum wire, and the reference electrode was an aqueous saturated calomel electrode, having in our working medium a difference of −0.385 V versus the $Fc^+|Fc$ couple (the intersolvental redox potential reference currently recommended by IUPAC).[54]

Photophysical Characterization. Steady-state fluorescence measurements to determine quantum efficiencies were performed on a Jobin-Yvon Fluorolog-3 spectrofluorometer equipped with double monochromator and a Xe lamp. Measurements of the fluorescence emission versus temperature were instead carried out on a Cary Eclipse (Varian Inc., Australia) spectrofluorometer, where the sample temperature can be controlled by a Peltier thermostatic system. Both instruments were equipped with a Hamamatsu R928P photomultiplier tube as detector. Emission spectra were corrected for the spectral sensitivity of the detection system by standard correction curves. The emission intensities were normalized to a nominal absorption value of 0.1. Quantum yields were determined by comparison with the emission of $[Ru(bipy)_3]Cl_2$ in aerated water (Φ = 0.04).[36] Lifetimes were measured in the frequency domain, as previously described.[55] In particular, dynamic fluorescence measurements were performed with a frequency-modulated phase fluorometer (Digital K2, I.S.S., Urbana, IL). The excitation was accomplished by the 9 mW output of a 378 nm diode laser (I.S.S., Urbana, IL). At least 15 data at logarithmically spaced frequencies in the range 0.3−30 MHz with a cross-correlation frequency of 400 Hz (A2D, ISS Inc., USA) have been acquired for lifetime measurements. Convenient accuracies for phase angles and modulation ratios have been 0.2° and 0.004, respectively. Lifetime measurements were performed under magic-angle conditions,[41] and a 535 nm long pass filter (Andover Co.) was employed in order to cut light scattering. A solution of glycogen in doubly distilled water was used as a reference sample.[56] Lifetime data fitting was accomplished by an ISS routine based on the Marquardt least-squares minimization, with at least a two-exponential decay scheme in order to take into account the scattering contribution to the overall signal. The fit of the fluorescence intensity decay $F(t)$ yields the lifetime values τ_i together with the corresponding fractional intensities f_i: $F(t) = \sum \alpha_i e^{-t/\tau_i}$ and $f_i = \alpha_i\tau_i/\sum \alpha_i\tau_i$, where α_i represents the pre-exponential factors.

TPE Measurements and Cellular Uptake. The laser source for TPE imaging was a mode-locked Ti:sapphire laser (Mai Tai HP, Spectra Physics, CA) with pulses of 120 fs full width at half-maximum and 80 MHz repetition frequency. The optical setup was built around a confocal scanning head (FV-300, Olympus, Japan) mounted on an upright optical microscope (BX51, Olympus, Japan) equipped with a high working distance objective (NA = 1.1, wd = 2 mm, 60×, water immersion, Olympus, Japan). The objective simultaneously focused the laser beam on the sample and collected the signal in epi-fluorescence geometry through the nondescanned (ND) collection unit described previously.[25] The signal reaching the ND-unit was spectrally resolved by a system of dichroic mirrors and band-pass filters and fed to three Hamamatsu photomultipliers (HC125-02, Hamamatsu, Japan). In the experiments reported here, the luminescence signal was collected through 485/50, 535/50, and 600/40 band-pass filters in order to separate the fluorescence light from undesired autofluorescence from the sample and to remove scattering radiation. TPE images have been processed by means of Fluoview 5.0 software (Olympus, Japan).

Cellular uptake experiments were performed on HEK-293, an immortal cell line, on B16 cells, a murine melanoma tumor cell line, and on primary macrophages. Primary macrophages were differentiated as previously described:[57] in brief, bone marrow precursors were freshly isolated from C57/BL6 mouse femurs and cultured for 7 days in the presence of M-CSF.

For all the experiments, 24 h before the measurements, 500 000 cells per well were plated on tissue 6-well plates in Dulbecco's modified Eagle's Medium (DMEM) supplemented with 10% heat-inactivated fetal calf serum, 2 mM L-Glutamine, andpenicillin−streptomycin (EuroClone), at 37 °C under a 5% CO_2 atmosphere. When needed, the culture medium was replaced with phosphate buffer solution (PBS) at pH 7.2−7.4 before the start of the measurements. A small aliquot of the probe (50 μL of 0.12 mM solution or 30 μL of 0.20 mM solution) was added to 2 mL of either PBS or DMEM (for the experiments requiring longer incubation time) in different wells of the plate. The fluorescence emission was recorded after the addition of the complex by exploiting two-photon excitation at 770 nm (with an excitation power of about 20 mW on the sample plane) through the ND unit as described above. The 512 × 512 pixel images shown in the paper are the result of 5 Kalman average scans with 10 μs of residence time per pixel. The field of view was variable between 460 × 460 and 184 × 184 μm^2, except for the enlargement in Figure 6, where the field of view was 39 × 39 μm^2, and it is reported in each figure caption.

■ ASSOCIATED CONTENT

Ⓢ Supporting Information

Figures showing the cyclic voltammetric analysis of **1**, the variable-temperature emission spectra of **2** and **3**, and TPE images of cell uptakes. This material is available free of charge via the Internet at http://pubs.acs.org.

AUTHOR INFORMATION

Corresponding Author

*E-mail: monica.panigati@unimi.it (M.P.); emanuela.licandro@unimi.it (E.L.).

Present Address

⊥Institute of Inorganic Chemistry, University of Zurich, Winterthurerstrasse 190, CH-8057 Zurich, Switzerland.

Notes

The authors declare no competing financial interest.

ACKNOWLEDGMENTS

We thank the Ministero dell'Istruzione, dell'Università e della Ricerca (MIUR, Rome), and the University of Milan, PRIN 2007 (2007F9TWKE_002) and PRIN 2009 (20093N774P_003), and CNR-Rome for financial support. We also thank Mrs. Marianna Greco and Mr. Daniele Sempio for some experimental work.

ABBREVIATIONS

Ac_2O, acetic anhydride; Boc, *tert*-butoxycarbonyl; DCC, dicyclohexylcarbodiimide; DCU, dicyclohexylurea; Cl-Cbz, 2-chlorobenzyloxycarbonyl; DMEM, Dulbecco's modified Eagle's Medium; HATU, *O*-(7-azabenzotriazol-1-yl)-*N*,*N*,*N*′,*N*′-tetramethyluronium hexafluorophosphate; ppd, 2,5-diphenyl-1,3,4-oxadiazole; MBHA, 4-methylbenzhydryl amine hydrochloride; MESNa, sodium mercaptoethanesulfonate; DIPEA, diisopropyl ethyl amine; NHE, standard hydrogen electrode; NMP, *N*-methylpyrrolidone; PBS, phosphate buffer solution; PNA, peptide nucleic acids; Py, pyridine; TFA, trifluoroacetic acid; TFMSA, trifluoromethanesulfonic acid; TPE, two-photon excitation

REFERENCES

(1) Jaouen, G.; Vessières, A. *Pure Appl. Chem.* **1985**, *57*, 1865−1874.

(2) Top, S.; Jaouen, G.; Vessières, A.; Abjean, J. P.; Davoust, D.; Rodger, C. A.; Sayer, B. G.; McGlinchey, M. J. *Organometallics* **1985**, *4*, 2143−2150.

(3) (a) Hillard, E. A.; Jaouen., G. *Organometallics* **2011**, *30*, 20−27. (b) *Bioorganometallics*; Jaouen, G., Ed.; Wiley-VCH: Weinheim, Germany, 2006.

(4) *Topics in Organometallic Chemistry*; Simonneaux, G., Ed.; Springer-Verlag: Berlin, Heidelberg, Germany, 2006; Bioorganometallic Chemistry Series Vol. *17*.

(5) Gasser, G.; Metzler-Nolte, N. *Curr. Opin. Chem. Biol.* **2012**, *16*, 84−91.

(6) Fernandez-Moreira, V.; Thorp-Greenwood, F. L.; Coogan, M. P. *Chem. Commun.* **2010**, *46*, 186−202.

(7) (a) Whrighton, M.; Morse, D. L. *J. Am. Chem. Soc.* **1974**, *96*, 998−1003. (b) Giordano, P. J.; Fredericks, S. M.; Whrighton, M.; Morse, D. L. *J. Am. Chem. Soc.* **1978**, *100*, 2257−2259.

(8) Moore, S. A.; Frazier, S. M.; Sibbald, M. S.; DeGraff, B. A.; Demas, J. N. *Langmuir* **2011**, *27*, 9567−9575.

(9) Lo, K. K-W.; Tsang, K. H. K.; Sze, K. S.; Chung, C. K.; Lee, T. K. M.; Zhang, K. Y.; Hui, W. K.; Li, C. K.; Lau, J. S. Y.; Ng, D. C. M.; Zhu, N. *Coord. Chem. Rev.* **2007**, *251*, 2292−2310.

(10) Balasingham, R. G.; Coogan, M.; Thorp-Greenwood, F. L. *Dalton Trans.* **2011**, *40*, 11663−11674.

(11) Amoroso, A. J.; Coogan, M. P.; Dunne, J. E.; Fernández-Moreira, V.; Hess, J. B.; Hayes, A. J.; Lloyd, D.; Millet, C. O.; Pope, S. J. A.; Williams, C. F. *Chem. Commun.* **2007**, 3066−3068.

(12) Lo, K. K-W.; Hui, W. K.; Chung, C. K.; Tsang, K. H-K.; Ng, D. C-M.; Zhu, N. Y.; Cheung, K. K. *Coord. Chem. Rev.* **2005**, *249*, 1434−1450.

(13) (a) Fernández-Moreira, V.; Thorp-Greenwood, F. L.; Amoroso, A. J.; Cable, J.; Court, J. B.; Gray, V.; Hayes, A. J.; Jenkins, R. L.; Kariuki, B. M.; Lloyd, D.; Millet, C. O.; Williams, C. F.; Coogan, M. P. *Org. Biomol. Chem.* **2010**, *8*, 3888−3901. (b) Louie, M.-W.; Liu, H. W.; Lam, M. H. C.; Lau, T. C.; Lo, K. K.-W. *Organometallics* **2009**, *28*, 4297−4307. (c) Lo, K. K.-W.; Louie, M.-W.; Sze, K.-S.; Lau, J. S.-Y. *Inorg. Chem.* **2008**, *47*, 602−611.

(14) *Peptide Nucleic Acids: Protocols and Applications*, 2nd ed.; Nielsen, P. E., Ed.; Horizon Bioscience: Wymondham, U.K., 2004.

(15) Gasser, G.; Sosniak, A. M.; Metzler-Nolte, N. *Dalton Trans.* **2011**, *40*, 7061−7076 and references cited therein.

(16) Singh, R.,P.; Oh, B−K.; Choi, J.-W. *Bioelectrochemistry* **2010**, *79*, 153−161.

(17) Wang, J. *Biosens. Bioelectron.* **1998**, *13*, 757−762.

(18) Metzler-Nolte, N. In *Bioorganometallics*; Jaouen., G., Ed.; Wiley-VCH: Weinheim, Germany, 2006; pp 125−180.

(19) (a) Baldoli, C.; Rigamonti, C.; Maiorana, S.; Licandro, E.; Falciola, L.; Mussini, P. *Chem. Eur. J.* **2006**, *12*, 4091−4100. (b) Baldoli, C.; Cerea, P.; Giannini, C.; Licandro, E.; Rigamonti, C.; Maiorana, S. *Synlett* **2005**, *13*, 1984−1994.

(20) Sforza, S.; Corradini, R.; Tedeschi, T.; Marchelli, R. *Chem. Soc. Rev.* **2011**, *40*, 221−232.

(21) Prencipe, G.; Maiorana, S.; Verderio, P.; Colombo, M.; Fermo, P.; Caneva, E.; Prosperi, D.; Licandro, E. *Chem. Commun.* **2009**, 6017−6019.

(22) Gasser, G.; Pinto, A.; Neumann, S.; Sosniak, A. M.; Seitz, M.; Merz, K.; Heumann, R.; Metzler-Nolte, N. *Dalton Trans.* **2012**, *41*, 2304−2313 and references therein.

(23) Xavier, C.; Giannini, C.; Dall'Angelo, S.; Gano, L.; Maiorana, S.; Alberto, R.; Santos, I. *J. Biol. Inorg. Chem.* **2008**, *13*, 1345−1349.

(24) Patra, M.; Gasser, G.; Bobukhov, D.; Merz, K.; Shtemenkob, A. V.; Metzler-Nolte, N. *Dalton Trans.* **2010**, *39*, 5617.

(25) Ferri, E.; Donghi, D.; Panigati, M.; Prencipe, G.; D'Alfonso, L.; Zanoni, I.; Baldoli, C.; Maiorana, S.; D'Alfonso, G.; Licandro, E. *Chem. Commun.* **2010**, *46*, 6255−6257.

(26) Panigati, M.; Mauro, M.; Donghi, D.; Mercandelli, P.; Mussini, P.; De Cola, L.; D'Alfonso, G. *Coord. Chem. Rev.* **2012**, *256*, 1621−1643.

(27) Donghi, D.; D'Alfonso, G.; Mauro, M.; Panigati, M.; Mercandelli, P.; Sironi, A.; Mussini, P.; D'Alfonso, G. *Inorg. Chem.* **2008**, *47*, 4243−4255.

(28) Mauro, M.; Quartapelle Procopio, E.; Sun, Y.; Chien, C. H.; Donghi, D.; Panigati, M.; Mercandelli, P.; Mussini, P.; D'Alfonso, G.; De Cola, L. *Adv. Funct. Mater.* **2009**, *19*, 2607−2614.

(29) Quartapelle Procopio, E.; Mauro, M.; Panigati, M.; Donghi, D.; Mercandelli, P.; Sironi, A.; D'Alfonso, G.; De Cola, L. *J. Am. Chem. Soc.* **2010**, *132*, 14397−14399.

(30) Mauro, M.; Yang, C.-H.; Shin, C.-Y.; Panigati, M.; Chang, C.-H.; D'Alfonso, G.; De Cola, L. *Adv. Mater.* **2012**, *24*, 2054−2058.

(31) Koppelhus, U.; Nielsen, P. E. *Adv. Drug Delivery Rev.* **2003**, *55*, 267−280.

(32) Oriskovich, T. A.; White, P. S.; Thorp, H. H. *Inorg. Chem.* **1995**, *34*, 1629−1631.

(33) Zobi, F.; Blacque, O.; Schmalle, H. W.; Spingler, B.; Alberto, R. *Inorg. Chem.* **2004**, *43*, 2087−2096.

(34) Zobi, F.; Spingler, B.; Alberto, R. *ChemBioChem* **2005**, *6*, 1397−1405.

(35) Mauro, M.; Panigati, M.; Donghi, D.; Mercandelli, P.; Mussini, P.; Sironi, A.; D'Alfonso, G. *Inorg. Chem.* **2008**, *47*, 11154−11165.

(36) Ishida, H.; Tobita, S.; Hasegawa, Y.; Katoh, R.; Nozaki, K. *Coord. Chem. Rev.* **2010**, *254*, 2449−2458.

(37) (a) Friedman, A. E.; Chambron, J. C.; Sauvage, J. P.; Turro, N. J.; Barton, J. K. *J. Am. Chem. Soc.* **1990**, *112*, 4960−4965. (b) Feeney, M. M.; Kelly, J. M.; Tossi, A. B.; Kirsch-de Mesmaeker, A.; Lecomte, J.-P. *J. Photochem. Photobiol. B: Biol.* **1994**, *23*, 69−78. (c) Moucheron, C.; Kirsch-de Mesmaeker, A.; Kelly, J. M. *J. Photochem. Photobiol. B: Biol.* **1997**, *40*, 91−106. (d) Le Gac, S.; Foucart, M.; Gerbaux, P.; Defrancq, E.; Moucheron, C.; Kirsch-de Mesmaeker, A. *Dalton Trans.* **2010**, *39*, 9672−2683.

(38) (a) Olmon, E. D.; Hill, M. G.; Barton, J. K. *Inorg. Chem.* **2011**, *50*, 12034−12044. (b) Olmon, E. D.; Sontz, P. A.; Blanco-Rodríguez,

A. M.; Towrie, M.; Clark, I. P.; Vlcek, A., Jr.; Barton, J. K. *J. Am. Chem. Soc.* **2011**, *133*, 13718−13730. (c) Yam, V. W. V.; Lo, K. K. W.; Cheung, K. K.; Kong, R. Y. C. *J. Chem. Soc., Dalton Trans.* **1997**, 2067−2072.
(39) Vlcek, A. A., Jr.; Dodsworth, S.; Pietro, W. J.; Lever, A. B. P. *Inorg. Chem.* **1995**, *34*, 1906−1913.
(40) Steenken, S.; Jovanovic, S. V. *J. Am. Chem. Soc.* **1997**, *119*, 617−618.
(41) See for instance the values of two of the empirical parameters used for measuring solvent polarity for water, acetonitrile, and DMSO, respectively. E_T = 63.1, 46.0, and 45.0: Reichardt, C. *Angew. Chem., Int. Ed. Engl.* **1979**, *18*, 98−110. π^* = 1.09, 0.75, and 1.00: Kamlet, M. J.; Abboud, J.-L- M.; Abraham, M. H.; Taft, R. W. *J. Org. Chem.* **1983**, *48*, 2877−2887.
(42) Lakowicz, J. R. *Principles of Fluorescence Spectroscopy*, 2nd ed., Kluver Academic/Plenum: New York, 1999.
(43) Coogan, M. P.; Fernandez-Moreira, V.; Hess, J. B.; Pope, S. J. A.; Williams, C. *New J. Chem.* **2009**, *33*, 1094−1099.
(44) (a) Petersson, B.; Nielsen, B. B.; Rasmussen, H.; Larsen, I. K.; Gajhede, M.; Nielsen, P. E.; Kastrup, J. S. *J. Am. Chem. Soc.* **2005**, *127*, 1424−1430. (b) Tomac, S.; Sarkar, M.; Ratilainen, T.; Wittung, P.; Nielsen, P. E.; Norden, B.; Gra1slund, A. *J. Am. Chem. Soc.* **1996**, *118*, 5544−5552.
(45) Vernille, J. P.; Kovell, L. C.; Schneider, J. W. *Bioconjugate Chem.* **2004**, *15*, 1314−1321.
(46) (a) Gurtovenko, A. A.; Anwar, J. *J. Phys. Chem. B* **2007**, *111*, 10453−10460. (b) Trubiani, O.; Salvolini, E.; Santoleri, F.; Arcangelo, C. D.; Spoto, G.; Di Primio, R.; Mazzanti, L. *J. Membr. Biol.* **2005**, *204*, 77−84.
(47) (a) Turner, Y.; Wallukat, G.; Saalik, P.; Wiesner, B.; Pritza, S.; Oehlkea, J. *J. Pept. Sci.* **2010**, *16*, 71. (b) Kaihatsu, K.; Huffman, K. E.; Corey, D. R. *Biochemistry* **2004**, *43*, 14340−14347. (c) Abes, S.; Williams, D.; Prevot, P.; Thierry, A.; Gait, M. J.; Lebleu, B. *J. Controlled Release* **2006**, *110*, 595−604.
(48) Yanai, H.; Ban, T.; Wang, Z. C.; Choi, M. K.; Kawamura, T.; Negishi, H.; Nakasato, M.; Lu, Y.; Hangai, S.; Koshiba, R.; Savitsky, D.; Ronfani, L.; Akira, S.; Bianchi, M. E.; Honda, K.; Tamura, T.; Kodama, T.; Taniguchi, T. *Nature* **2009**, *462*, 99−103.
(49) (a) New, E. J.; Parker, D. *Org. Biomol. Chem.* **2009**, *7*, 851−855. (b) New, E. J.; Parker, D.; Smith, D. G.; Walton, J. W. *Curr. Opin. Chem. Biol.* **2010**, *14*, 238−246.
(50) O'Connor, N. A.; Stevens, N.; Samaroo, D.; Solomon, M. R.; Marti, A. A.; Dyer, J.; Vishwasrao, H.; Atkins, D. L.; Kandel, E. R.; Turro, N. J. *Chem. Commun.* **2009**, 2640−2642.
(51) The bridging coordination of the halides is so stable that the synthesis of $[Re_2(CO)_6(\mu\text{-}X)_2(\mu\text{-diazine})]$ complexes with X ligands different from halides (such as OR^- and SR^-) required a different route, using starting materials not containing halides.[52] This strongly excludes halides being replaced by hydroxides or carboxylates in the cellular media.
(52) Raimondi, A.; Panigati, M.; Maggioni, D.; D'Alfonso, L.; Mercandelli, P.; Mussini, P.; D'Alfonso, G. *Inorg. Chem.* **2012**, *51*, 2966−2975.
(53) Bard, A. J.; Faulkner, L. R. In *Electrochemical Methods. Fundamentals and Applications*; Wiley: New York, 2002; pp 648−650.
(54) (a) Gritzner, G.; Kuta, J. *Pure Appl. Chem.* **1984**, *56*, 461−466. (b) Gritzner, G. *Pure Appl. Chem.* **1990**, *62*, 1839−1858.
(55) Panigati, M.; Donghi, D.; D'Alfonso, G.; Mercandelli, P.; Sironi, A.; D'Alfonso, L. *Inorg. Chem.* **2006**, *45*, 10909−10921.
(56) Collini, M.; Chirico, G.; Baldini, G.; Bianchi, M. E. *Biopolymers* **1995**, *36*, 211−225.
(57) Zanoni, I.; Ostuni, R.; Capuano, G.; Collini, M.; Caccia, M.; Ronchi, A. E.; Rocchetti, M.; Mingozzi, F.; Foti, M.; Chirico, G.; Costa, B.; Zaza, A.; Ricciardi-Castagnoli, P.; Granucci, F.. *Nature* **2009**, *460*, 264−268.